Biogeosciences Discuss., 12, 14647–14692, 2015
www.biogeosciences-discuss.net/12/14647/2015/
doi:10.5194/bgd-12-14647-2015

Biogeosciences
Discussions
Open Access

Responses of two nonlinear microbial models to warming or increased carbon input

Y. P. Wang[1], J. Jiang[2], B. Chen-Charpentier[3], F. B. Agusto[4], A. Hastings[5], F. Hoffman[6], M. Rasmussen[7], M. J. Smith[8], K. Todd-Brown[9,11], Y. Wang[10], X. Xu[9], and Y. Q. Luo[9]

[1]CSIRO Ocean and Atmosphere, PMB 1, Aspendale, Victoria 3195, Australia
[2]Department of Ecology and Evolutionary Biology, University of Tennessee, Knoxville, TN37996, USA
[3]Department of Mathematics, University of Texas, Arlington, Texas, USA
[4]Department of Mathematics and Statistics, Austin Peay State University, Clarksville TN37044, USA
[5]Department of Environmental Science and Policy, University of California, One Shields Avenue, Davis, CA 95616, USA
[6]Oak Ridge National Laboratory, Computational Earth Sciences Group, P.O. Box 2008, Oak Ridge, TN 37831, USA
[7]Department of Mathematics, Imperial College, London, UK
[8]Computational Science Laboratory, Microsoft Research, Cambridge, UK

[9]Department of Microbiology and Plant Biology, University of Oklahoma, Norman, Oklahoma, USA
[10]Department of Mathematics, University of Oklahoma, Norman, Oklahoma, USA
[11]Pacific Northwest National Laboratory, Richland, Washington, USA

Received: 14 July 2015 – Accepted: 18 August 2015 – Published: 7 September 2015

Correspondence to: Y. P. Wang (yingping.wang@csiro.au)

Published by Copernicus Publications on behalf of the European Geosciences Union.

Abstract

A number of nonlinear microbial models of soil carbon decomposition have been developed. Some of them have been applied globally but have yet to be shown to realistically represent soil carbon dynamics in the field. Therefore a thorough analysis of their key differences will be very useful for the future development of these models. Here we compare two nonlinear microbial models of soil carbon decomposition: one is based on reverse Michaelis-Menten kinetics (model A) and the other on regular Michaelis-Menten kinetics (model B). Using a combination of analytic solutions and numerical simulations, we find that the oscillatory responses of carbon pools model A to a small perturbation in the initial pool sizes have a higher frequency and damps faster than model B. In response to soil warming, soil carbon always decreases in model A; but likely decreases in cool regions and increases in warm regions in model B. Maximum CO_2 efflux from soil carbon decomposition (F_{max}) after an increased carbon addition decreases with an increase in soil temperature in both models, and the sensitivity of F_{max} to the amount of carbon input increases with soil temperature in model A; but decreases monotonically with an increase in soil temperature in model B. These differences in the responses to soil warming and carbon input between the two nonlinear models can be used to differentiate which model is more realistic with field or laboratory experiments. This will lead to a better understanding of the significance of soil microbial processes in the responses of soil carbon to future climate change at regional or global scales.

1 Introduction

Dynamics of soil carbon in most global biogeochemical models are represented using first-order kinetics, which assumes that the decay rate of soil carbon is proportional to the size of soil carbon pool. This approach has been recently questioned on theoretical grounds (Schimel and Weintraub, 2003; Fontaine and Barot, 2005), and in the observed responses of soil carbon decay to addition of fresh organic litter (Fontaine et al., 2004; Sayer et al., 2011) or soil warming (Luo et al., 2001; Mellilo et al., 2002; Bradford et al., 2008). As a result, a number of nonlinear soil microbial models have been developed (Allison et al., 2010; Manzoni and Porporato, 2007; Wutzler and Reichstein, 2008), and a few of them have also been applied at global scales (Wieder et al., 2013; Sulman et al., 2014). Predictions of future soil carbon change by these nonlinear models can differ significantly from conventional linear models (Fontaine et al., 2007; Wieder et al., 2013). For example, conventional linear soil carbon models predict that soil carbon will decrease with global warming, all else being equal (Jenkinson et al., 1991), whereas the nonlinear models predict that the soil carbon can decrease or increase, depending on the temperature sensitivity of microbial growth efficiency and turnover rates (Frey et al., 2013; Hagerty et al., 2014; Li et al., 2014). However the nonlinear models have yet to be validated against field measurements as extensively as the conventional linear soil carbon models (Wieder et al., 2015), and have some undesirable features, such as the presence of strong oscillations or bifurcation (Manzoni and Porporato, 2007; Wang et al., 2014). Therefore it is important for us to improve our understanding of the behaviour of these nonlinear models before they are used in earth system models for informing climate decisions.

Nonlinear microbial models can explain why decomposition rate of recalcitrant organic soil carbon varies after the addition of easily decomposable organic carbon to soil, or priming effect (Kuzyakov, Friedel and Stahr, 2000). This response has been observed in the field (Fontaine et al., 2004; Sayer et al., 2011), but cannot predicted by conventional linear soil carbon models without modification (Fujita, Witte and Bodegom, 2014). Theoretically, decomposition of soil organic carbon is catalysed by extracellular enzymes that are produced by soil microbes, and the production rate of extracellular enzymes depends on biomass and composition of soil microbial population and their local environment. Therefore the decomposition rate of soil organic carbon should depend on both microbial biomass and substrate concentration (Schimel and Weintraub, 2003), rather than on substrate concentration only, as assumed in conventional linear models.

This sensitivity of decomposition of soil carbon to the input of additional carbon has important implications for the sink capacity of the land biosphere in global carbon cycle and carbon-climate feedback studies, because soil is the largest carbon pool in land biosphere with the longest residence time, and the magnitude of positive carbon-climate feedback strongly depend on the responses of soil carbon to future warming and changing carbon input (Jones and Fallow, 2009; Hargety et al., 2014).

A number of nonlinear models have been developed (Parnas, 1978; Smith, 1979; Schimel and Weintraub, 2003; Wutzler and Reichstein, 2008; Allison et al., 2010; Grant, 2014; Riley et al., 2014; Tang and Riley, 2014). Parnas (1979) explored the mechanism of priming effect using a nonlinear soil microbial model including both soil carbon and nitrogen dynamics. Smith (1979) developed a nonlinear model of soil carbon decomposition including the interactions among carbon, nitrogen, phosphorus and potassium. Smith's model represented multiple forms of carbon, nitrogen and phosphorus and their transformation via abiotic (such as adsorption and desorption) and biological processes by different groups of soil microbes. The soil models developed by both Parnas (1978) and Smith (1979) were based on regular Michaelis-Menten kinetics, or the rate of carbon decomposition depends linearly on the concentration of soil enzymes and nonlinearly on substrate concentration. This was challenged by Schimel and Weintraub (2003) who emphasized the importance of exoenzyme limitation on soil carbon decomposition. Schimel and Weintraub (2003) used a reverse Michaelis-Menten kinetics to show that the response of soil carbon decomposition to carbon substrate concentration can be nonlinear regardless of carbon supply. The reverse Michaelis-Menten kinetics for soil carbon decomposition assumes that the rate of carbon decomposition depends nonlinearly on enzyme concentration, and linearly on substrate concentration.

Using numerical simulations, various studies used those nonlinear models to explore the fundamental mechanisms controlling soil carbon decomposition (Schimel and Weintraub, 2003 for example), or sensitivity of soil carbon and other biogeochemical

Title Page
Abstract Introduction
Conclusions References
Tables Figures
◀| |▶
◀ ▶
Back Close
Full Screen / Esc
Printer-friendly Version
Interactive Discussion

processes to warming (Grant, 2014; Tang and Riley, 2014), or response of soil carbon to a small perturbation, such as priming (Wutzler and Reichsentein, 2013) and global change (Wieder et al., 2013; Sulman et al., 2014). Only few studies explored the mathematical properties of these nonlinear systems analytically, such as dynamic bifurcations, oscillation (Manzoni et al., 2004; Manzoni and Porporato, 2007; Raupach, 2007; Wang et al., 2014 for example).While numerical analyses have provided insights for particular models, results are likely specific to the models and the parameter values they used.

This study will use analytic tools to understand the mathematical properties of nonlinear microbial models. For simplicity and analytic convenience, we choose two simple types of nonlinear microbial models: one with regular Michaelis-Menten kinetics and other with the reverse Michaelis-Menten kinetics. We only use three pools for each type model and ignore the abiotic processes that can be quite important under certain conditions (see Tang and Riley, 2014 for an example). We will address the following questions: (1) how do the responses of these two models to soil warming differ and why? (2) Can both model simulate the response of soil carbon decomposition to increased carbon input as in a litter manipulation or laboratory priming experiment and what determines the magnitude of the response in each model?

2 Methods

2.1 Model description

Here we analyze two nonlinear soil microbial models: one model, model A, uses reverse Michaelis-Menten kinetics and the other, model B, uses regular Michaelis-Menten kinetics. Both models have three carbon pools: litter carbon, microbial biomass and soil carbon.

Model A is based on a nonlinear microbial model of soil carbon as described Wutzler and Reichstein (2013) (their model A1). The original model as described by Wutzler and Reichstein (2013) has four pools. Their dynamics is described as follows:

$$\frac{dC_l}{dt} = (1-a)F_{npp} - \mu_l C_l \frac{C_b}{C_b + K_b}, \tag{1}$$

$$\frac{dC_s}{dt} = aF_{npp} + \mu_b C_b - \mu_s C_s \frac{C_b}{C_b + K_b}, \tag{2}$$

$$\frac{dC_b}{dt} = \varepsilon \mu_m C_b \frac{C_m}{C_m + K_m} - \mu_b C_b, \tag{3}$$

and

$$\frac{dC_m}{dt} = (\mu_l C_l + \mu_s C_s)\frac{C_b}{C_b + K_b} - \mu_m C_b \frac{C_m}{C_m + K_m}, \tag{4}$$

where t is time in year, C_l, C_s, C_b and C_m represent the pool sizes of litter carbon, soil carbon, microbial biomass carbon and assimilable soil carbon in $g\,C\,m^{-2}$, respectively; F_{npp} is carbon input in $g\,C\,m^{-2}\,year^{-1}$, with a fraction of a going to soil carbon pool, and $(1-a)$ to litter carbon pool. μ_l, μ_s, μ_b and μ_m are turnover rates of litter carbon, soil carbon, microbial biomass and assimilable carbon in $year^{-1}$, respectively; ε is microbial growth efficiency, K_b and K_m are two empirical constants in $g\,C\,m^{-1}$ for the dependence of consumption of litter carbon or assimilable carbon by soil microbes on soil microbial biomass and assimilable carbon.

Because we are interested in the responses at time scale greater than 1 year, we assume that C_m is at steady state ($dC_m/dt = 0$) all the time because of its relatively fast turnover (< a few days). Therefore dynamics of microbial biomass, C_b, can be simplified to

$$\frac{dC_b}{dt} = \varepsilon(\mu_l C_l + \mu_s C_s)\frac{C_b}{C_b + K_b} - \mu_b C_b. \tag{5}$$

Model A as used in this paper consists of Eqs. (1), (2) and (5) unless otherwise specified. The type of kinetics was also used in the studies by Schimel and Weintraub (2003); Drake et al. (2013); Sulman et al. (2014).

The other nonlinear soil microbial carbon model used was based on the model used by Allison et al. (2010) and Wieder et al. (2013). The equations for model B are

$$\frac{dC_l}{dt} = (1-a)F_{npp} - C_b\frac{V_lC_l}{C_l+K_l}, \tag{6}$$

$$\frac{dC_s}{dt} = aF_{npp} + \mu_bC_b - C_b\frac{V_sC_s}{C_s+K_s}, \tag{7}$$

and

$$\frac{dC_b}{dt} = \varepsilon C_b\left(\frac{V_lC_l}{C_l+K_l} + \frac{V_sC_s}{C_s+K_s}\right) - \mu_bC_b, \tag{8}$$

where K_l and K_s are Michaelis-Menten constants in $\mathrm{g\,C\,m^{-2}}$, V_l or V_s are maximum rates of substrate carbon (litter or soil) assimilation rate per unit microbial biomass per year. This type of kinetics was used by Riley et al. (2014), Wieder et al. (2014) and Wang et al. (2014).

These two models make different assumptions about the rate-limiting step in carbon decomposition. Carbon decomposition is assumed to be limited by the number of binding sites or the amount of substrate in model A (Schimel and Weintraub, 2003), and by the enzyme activities or microbial biomass in model B (Allison et al., 2010). As a result, their dynamics and responses to a step change in external environmental can be quite different.

When carbon input, F_{npp} is equal to zero, the steady state solution is zero for litter and soil carbon pools for both models (a trivial solution). When $F_{npp} < 0$, the steady state solutions to Model A are:

$$C_l^* = \frac{(1-\alpha)F_{npp}}{\mu_l} + \frac{(\varepsilon^{-1}-1)(1-\alpha)\mu_bK_b}{\mu_l}, \tag{9}$$

$$C_b^* = \frac{F_{npp}}{(\varepsilon^{-1}-1)\mu_b}, \tag{10}$$

and

$$C_s^* = \left(a + \frac{1}{\varepsilon^{-1} - 1}\right) \frac{F_{npp}}{\mu_s} + \left(1 + a\left(\varepsilon^{-1} - 1\right)\right) \frac{\mu_b K_b}{\mu_s}. \tag{11}$$

The steady state solutions to model B are:

$$C_l^* = \frac{K_l}{\frac{\varepsilon V_l}{(1-\varepsilon)(1-a)\mu_b} - 1}, \tag{12}$$

$$C_b^* = \frac{F_{npp}}{\mu_b\left(\varepsilon^{-1} - 1\right)}, \tag{13}$$

and

$$C_s^* = \frac{K_s}{\frac{V_s}{\mu_b}\frac{\varepsilon}{\varepsilon + a(1-\varepsilon)} - 1} \tag{14}$$

CO_2 efflux from the decomposition of soil organic carbon (F_s), are calculated as:

$$F_s = (1 - \varepsilon)\,\mu_s C_s \frac{C_b}{C_b + K_b} \tag{15}$$

for model A and

$$F_s = (1 - \varepsilon)\,C_b \frac{V_s C_s}{C_s + K_s} \tag{16}$$

for model B.

2.2 Parameter values

Except parameter a, we allow all other model parameters to vary with soil temperature (T_s). Based on the work of Allison et al. (2010) and Hagerty et al. (2014), we used the following equations to describe the temperature dependence of those model parameters. They are:

$$\varepsilon = \varepsilon_R - x(T_s - T_R), \tag{17}$$

and

$$\mu_b = \mu_{bR} \exp(b(T_s - T_R)) \tag{18}$$

for both models. Where T_R is reference soil temperature in °C (= 15 °C), ε_R and μ_{bR} are the values of ε and μ_b at $T_s = T_R$, respectively, x and b are two empirical constants (see Table 1 for their default values).

There has been a debate about the temperature sensitivities of ε and μ_b (see Frey et al., 2013; Hargety et al., 2014). The microbial models as developed by Allison et al. (2010), and used by Wieder et al. (2013) and Wang et al. (2014) assumed that ε was temperature-sensitive and μ_b was temperature-insensitive (or $b = 0$). This assumption was recently challenged by Hargety et al. (2014) who found that μ_b was temperature sensitive and ε was temperature insensitive, based on a soil warming experiment in the laboratory. Here we will explore the consequence of different assumptions about the temperature sensitivities of ε and μ_b on the response of soil carbon to warming (see Sect. 3.2).

We also assume that three additional model parameters in model A, K_b, μ_l and μ_s depends on soil temperature exponentially. They are:

$$K_b = K_{bR} \exp(\alpha_k(T_s - T_R)), \tag{19}$$

$$\mu_l = \mu_{lR} \exp(\alpha_l(T_s - T_R)), \tag{20}$$

and

$$\mu_s = \mu_{sR} \exp(\alpha_s (T_s - T_R)) \tag{21}$$

where K_{bR}, μ_{lR} and μ_{sR} are the values of K_b, μ_l and μ_s when soil temperature (T_s) is equal to the reference temperature, T_R (= 15 °C in this study), and α_k, α_l and α_s are three empirical constants with their default values listed in Table 1.

For model B, we assumed that K_l, K_s, V_l and V_s increase with soil temperature exponentially. That is:

$$K_l = K_{lR} \exp(\beta_{kl} (T_s - T_R)), \tag{22}$$

$$K_s = K_{sR} \exp(\beta_{ks} (T_s - T_R)), \tag{23}$$

and

$$V_l = V_{lR} \exp(\beta_{vl} (T_s - T_R)), \tag{24}$$

$$V_s = V_{sR} \exp(\beta_{vs} (T_s - T_R)) \tag{25}$$

where K_{lR}, K_{sR}, V_{lR} and V_{sR} are the values of K_l, K_s, V_l, and V_s at reference soil temperature (T_R), respectively; and β_{kl}, β_{ks}, β_{vl} and β_{vs} are four empirical constants for model B (see Table 1).

As found by Wang et al. (2014), the microbial biomass as simulated by model B using the parameter values of Wieder et al. (2013) was quite low (< 1 % of total soil carbon), we therefore reduced the turnover rate of microbial biomass to 1.1 year^{-1} in this study by assuming that 2 % of total soil organic carbon is microbial biomass carbon at a soil temperature of 15 °C. Parameter values in model A at the reference temperature were obtained by calibrating the equilibrium carbon pool sizes against those from model B for a soil temperature of 15 °C and carbon input of 400 g C m^{-2} year^{-1}, as used in Wang et al. (2014).

2.3 Analytic solutions and numerical simulations

In this study, we used analytic solutions whenever possible for analyzing the mathematical properties of the two models in terms of the responses of carbon pools to a small perturbation, soil warming or an increased carbon input. Specifically, we analyzed the temperature of steady state soil carbon pool size (Eq. 11) to solve for the soil temperature at which equilibrium soil carbon is minimum, and derived approximate solutions to maximum CO_2 loss from soil carbon decomposition after the increased carbon input for each model (F_{max}). When analytic solution is not possible or too cumbersome, we used numerical simulations to show the differences between the two models in the responses of carbon pools to a small perturbation in litter or microbial carbon pool sizes, and the responses of CO_2 efflux from soil carbon decomposition to litter addition at a tropical forest site, or the responses of F_{max} to different combinations of soil temperature and carbon input rate.

3 Results

To understand how the responses of the two models to a step change in soil temperature or carbon input differ, we analysed some key properties of the responses of the two models to a small perturbation, i.e. whether both models oscillate in response to a small change in pool size and what determines the period and amplitude of the oscillation. Response of model B to perturbation has been analysed by Wang et al. (2014), and will not be elaborated here, only the period and amplitude are compared with those of model A.

3.1 Comparison of perturbation responses of two models

Perturbation analysis is a standard mathematical technique for analysing the behaviour of a dynamic system near their equilibrium states (see Drazin, 1992 for further details). There are two kinds of perturbation responses: stable or unstable. The system states, or carbon pool sizes in our case will always approach their equilibrium states for a stable response, or otherwise for an unstable response. For both stable and unstable responses, the transient change of a carbon pool size over time can be oscillatory or monotonic. As shown in Appendix A, the response of a carbon pool to a small perturbation always is stable for model A, and the response over time will be oscillatory only if $F_{\mathrm{npp}} < 4\frac{(1-\varepsilon)^2}{\varepsilon}\frac{\mu_{\mathrm{l}}\mu_{\mathrm{b}}^2 K_{\mathrm{b}}}{(\mu_{\mathrm{b}}-\mu_{\mathrm{l}})^2}$, or monotonic otherwise. This region of oscillation in the two-dimensional space of carbon input and soil temperature is shown in black in Fig. 1. Therefore the response of model A to a small perturbation is oscillatory under most conditions (soil temperature within 10 and 30 °C) experienced by terrestrial ecosystems.

Results of perturbation analysis are applicable only when perturbation is small in general, but are good approximations for any realistic perturbation for our two models in this study (see Appendix A of this paper, and Appendix B in Wang et al., 2014). Therefore we can predict how soil carbon or other carbon pools change over time in response to a change in carbon input or soil warming (i.e. a perturbation of external environment) and explain why the responses of the carbon pools are different between the two models.

To illustrate how the responses of carbon pools to a small perturbation differ between the two models, we numerically simulated the recovery of all three carbon pools in each model after a 10 % reduction at time $t = 0$ in both litter and microbial carbon from their respective steady state values, while no perturbation was applied to soil carbon at $t = 0$ (see Fig. 2). The amplitude of the initial oscillation is about 70 g C m^{-2} for litter pool (see Fig. 2b) and 7 g C m^{-2} for the microbial carbon (see Fig. 2d) in model B, as compared to about 25 g C m^{-2} (see Fig. 2a) for the litter pool and 4 g C m^{-2} for the microbial pool (see Fig. 2c) in model A. Both the litter and microbial carbon pools are very close to their respective steady state values in model A, but continue to oscillate in model B after 20 years.

The oscillatory response can be mathematically characterized by half-life ($t_{0.5}$) and period (p). For a stable oscillatory response, the amplitude of oscillation decays exponentially. The time for the amplitude to reach 50 % of its initial value at $t = 0$ is defined as half-life time ($t_{0.5}$). The smaller $t_{0.5}$ is the faster the oscillation damps. As explained in the Appendix A, values of $t_{0.5}$ and p of model A are much smaller than model B for a given soil temperature and perturbation, that is why the oscillatory responses of model A damp much faster than model B.

There are significant differences in the response of soil carbon between the two models. While there is no response of soil carbon to a small perturbation in initial sizes of litter carbon and microbial biomass in model B, soil carbon in model A decreases initially to a minimum value at 5 years after the perturbation, then gradually increases to its steady state value. These differences in the response of soil carbon between the two models can be explained by the differences in the structure of eigenvectors for litter carbon and microbial biomass between the two models (see Appendix A for further details).

3.2 Minimum soil carbon temperature

Here we explore how soil carbon responds to an instant step increase in soil temperature, as in many soil warming experiments (Luo et al., 2001; Mellilo et al., 2002), and we ignore the response of carbon input to warming.

As explained in Appendix A, the response of soil carbon to warming always is stable in both models, and is likely to be weakly oscillatory in model A and monotonic in model B, and the transient change in soil carbon can be predicted using the generalised solution to soil carbon for each model (see Appendix A). Therefore the directional change of soil carbon in response to warming, i.e. increasing or decreasing only depends on the sensitivity of equilibrium soil carbon pool to soil temperature in both models.

As shown in Appendix B, the equilibrium pool size of soil carbon of model A always decreases with soil warming if carbon input does not increase with warming. For model B, the equilibrium pool size of soil carbon can increase or decrease in response to warming, depending on soil temperature and model parameter values. In

Appendix B, we showed that a soil temperature (T_x) may exist at which the equilibrium soil carbon is minimum. Identifying T_x is important for predicting the directional change of soil carbon in a warmer world, because soil carbon will decrease if the warmed soil temperature is below T_x, and increase otherwise.

The minimum soil carbon temperature, T_x, depends on three model parameters: the fraction of carbon input directly into the soil pool (a), microbial biomass turnover rate (μ_b or its temperature sensitivity b) and microbial growth efficiency (ε or its temperature sensitivity x). Figure 3a shows that T_x decreases with an increase in a or x. When $x < 0.005\,^\circ\mathrm{C}^{-1}$ and $a < 0.5$, T_x is $> 40\,^\circ\mathrm{C}$ or soil carbon in model B will decrease with warming when the warmed soil temperature is below 40 °C; when $a > 0.4$ and x $> 0.02\,^\circ\mathrm{C}^{-1}$, T_x is $< 0\,^\circ\mathrm{C}$ (the black region on the top left corner of Fig. 3a), or soil carbon in model B will increase with warming if the warmed soil temperature is above 0 °C.

Figure 3b shows that T_x decreases with an increase in b or x. When the turnover rate of microbial biomass is not sensitive to soil temperature ($b = 0$) and $x = 0.016\,^\circ\mathrm{C}^{-1}$ as the default values used for model B, T_x is about 35 °C. When $b = 0.063$ as estimated Hagerty et al. (2014), T_x does not exist, irrespective of the value of x, therefore the equilibrium soil carbon pool size always increases with soil warming.

Therefore the equilibrium soil carbon pool size always decreases with soil warming in model A, but can increase or decrease in model B, depending on its temperature sensitivities of microbial growth efficiency and microbial turnover rate and the fraction of carbon input entering soil carbon pool directly.

3.3 Response of soil carbon to an increased litter input

Here we compare the simulated responses of soil carbon to litter addition by the two models with field measurements from an experiment as described by Sayer et al. (2011). The experiment used three treatments: increased litter input (L^+) with additional litter from the litter removal treatment, litter remove (L^-) with aboveground litter being removed regularly, and control (C). Measurements of CO_2 efflux from soil were made, and the contribution of root-rhizosphere respiration to soil respiration was estimated using $\delta^{13}C$ technique. Sayer et al. (2011) found that the CO_2 efflux from the decomposition of soil organic carbon in the L^+ treatment was 46 % higher than in the control, therefore increased litter addition accelerated the decomposition of soil organic carbon. Here we assess whether the observed response of soil carbon decomposition to increased litter input can be reproduced by both models.

Inputs to each model including the monthly data of soil temperature, soil moisture, litter input from 2002 to 2008 for two treatments (C and L^+) at the site were compiled from Sayer, Power and Tanner, (2007), Sayer and Tanner (2010a, b) (see Fig. 4 for monthly litter input as an example). We also assumed that the contribution of fine-root respiration to total soil respiration (root respiration plus heterotrophic respiration) was 35 % for the control treatment and 21 % for the litter addition treatment, based on the estimates by Sayer et al. (2011).

The initial sizes of all pools were obtained by running each model by reusing the monthly input for the first two years until all pools reached steady state (i.e. the change is pool size between two successive cycle is less than 0.01 %).

Using the initial pool sizes for each model and the monthly input from 2002 to 2008, we numerically integrated both models and calculated the average contributions to total soil CO_2 efflux from the decomposition of litter and soil organic carbon for the last 2 years (2007–2008), and compared the simulated results with the estimates from field measurements by Sayer et al. (2011).

The simulated initial microbial biomass carbon by both models is 240 g C m^{-2}, which is very close to the measured microbial biomass carbon of 219 g C m^{-2} by Sayer et al. (2007). The simulated initial soil carbon is 6715 for model A and 6945 g C m^{-2} for model B, which is higher than the estimated soil carbon of 5110 g C m^{-2} in the top 25 cm (Cavelier et al., 1992) and lower than the estimated soil carbon of 9272 g C m^{-2} in the top 50 cm soil (Grimm, 2007).

The estimated total soil CO_2 efflux from the control treatment by Sayer et al. (2011) was 1008 $g\,C\,m^{-2}\,year^{-1}$ from 2007 to 2008, which was closely simulated by both models (1004 $g\,C\,m^{-2}\,year^{-1}$ by model A and 1008 $g\,C\,m^{-2}\,year^{-1}$ by model B). However both models overestimated the total soil CO_2 efflux from the litter addition treatment. The estimated efflux by Sayer et al. (2011) was 1380 $g\,C\,m^{-2}\,year^{-1}$, as compared with the simulated flux of 1425 by model A and 1502 $g\,C\,m^{-2}\,year^{-1}$ by model B (see Fig. 5).

The additional CO_2 efflux from the decomposition of soil carbon in the litter addition treatment was estimated to be 180 ± 50 $g\,C\,m^{-2}\,year^{-1}$ by Sayer et al. (2011), which was quite well simulated by model B (105 $g\,C\,m^{-2}\,year^{-1}$) (see Fig. 5b), but was underestimated by model A (29 $g\,C\,m^{-2}\,year^{-1}$) (see Fig. 5a).

The difference in the simulated response of soil organic carbon decomposition to the increased litter input by two models can be explained by differences in their Michaelis-Menten kinetics. The rate of carbon loss from the decomposition of soil carbon depends on both soil carbon and microbial biomass in both models. Because soil carbon is unlikely to change significantly within a few years, the rate of CO_2 emission from soil carbon decomposition will largely depend on microbial biomass, and that dependence is nonlinear following the reverse Michaelis-Menten equation in model A (see Eq. 2), and is linear in model B (see Eq. 7). Therefore the simulated response of soil organic carbon decomposition to increased litter input by model B is more sensitive to microbial biomass, and is higher than that by model A.

3.4 Response to priming: maximum CO_2 efflux from soil carbon decomposition

Results from the above comparison of the responses of two models to the increased litter input are likely dependent on soil temperature, carbon input, and model parameter values. To understand the differences of the responses of two models to litter addition across a range of carbon inputs and soil temperatures at any parameter values, we use the analytic approximations to maximum CO_2 efflux from the priming treatment for each model to identify key differences in their response to priming.

Priming is defined as the change of organic carbon decomposition rate after addition of easily decomposable organic substance to soil (Kuzyakove, Friedel and Stahr, 2000). In lab priming experiments, a given amount of isotopically labelled C substrate is added to the primed treatment only at the beginning of the experiment ($t = 0$), and no substrate is added to the control. CO_2 effluxes from soil carbon decomposition are estimated from measurements for the following weeks or longer (Cheng et al., 2014). The effect of priming, p, is calculated as $(R_p - R_c)/R_c$, where R_c and R_p are the CO_2 efflux from the decomposition of soil organic carbon in the control and primed treatments, respectively. Maximum values of p are usually reported in most priming studies (see Cheng et al., 2014).

However analytic approximations to p for both models are quite cumbersome for analysing their differences in the responses to priming. Another way to quantify the priming effect is the maximum CO_2 efflux from soil organic carbon decomposition after carbon addition at time $t = 0$ from the primed treatment (Jenkinson et al., 1985; Kuzyakova, Friedelb and Stahr, 2000).This quantity can be easily measured in the laboratory or field.

In both models, the equilibrium soil microbial biomass is proportional to carbon input (see Eqs. 11 and 13). In the primed treatment, the amount of carbon added at $t = 0$ usually is well above the rate of the carbon input under natural conditions, and no further carbon is added at $t > 0$. Therefore the microbial biomass will increase until reaching a maximum value, then decreases with time after $t = 0$.

As shown in Appendix C, the maximum CO_2 efflux from soil carbon decomposition in the primed treatment, F_{max}, is a function of maximum microbial biomass after $t = 0$, microbial growth efficiency and soil carbon turnover rate for model A (see Eq. C11 for F_A in Appendix C), and maximum microbial biomass, microbial growth efficiency and microbial turnover rate after $t = 0$ for model B (see Eq. C14 for F_B).

Figure 6 shows that F_max (or F_A for model A, F_B for model B) increases with carbon input, and decreases with an increase in soil temperature for both models.

However the sensitivity of F_max to carbon input at different soil temperatures is different between the two models. For model A, the sensitivity of F_max to carbon input is greatest around a soil temperature of 25 °C, and is quite small at a soil temperature $< 5\,^\circ$C. For model B, the sensitivity of F_max to carbon input decreases with an increase in soil temperature (see Fig. 6).

The sensitivity of F_max to soil temperatures in both models can be explained by the analytic approximations (Eq. C11 for model A and C14 for model B). Maximum CO_2 efflux is proportional to soil carbon in model A, and to the maximum microbial biomass in model B, both soil carbon and maximum microbial biomass in both models decrease with an increase in soil temperature for the parameter values we used (see Fig. 6c), therefore F_max also decreases with an increase in soil temperature.

Differences in the sensitivity of F_max to carbon input at different soil temperatures in the two models can also be explained by their respective analytic approximation. In model A, F_A nonlinearly varies with maximum microbial biomass (see Eq. C11), which is proportional to carbon addition at $t = 0$ ($\Delta\mathrm{C}_\mathrm{l}$) and varies nonlinearly with the initial pool size of microbial biomass (C_b^*) (see Eq. C10). Therefore the sensitivity of F_A to $\Delta\mathrm{C}_\mathrm{l}$ varies with $\Delta\mathrm{C}_\mathrm{l}$ itself and C_b^* nonlinearly, or the sensitivity is larger at a smaller value of C_b^*. For a given F_npp, C_b^* decreases with an increase in soil temperature. At high soil temperature, C_b^* is low (see Fig. 6c), therefore sensitivity to maximum microbial biomass and carbon input is high (see Fig. 6a).

In model B, sensitivity of F_B to carbon input is determined by maximum microbial biomass ($\mathrm{C}_\mathrm{bmax,B}$) that varies with equilibrium litter pool size (C_l^*) following the regular Michaelis-Menten equation ($\mathrm{C}_\mathrm{bmax,B} \propto M_\mathrm{l}$ in Eq. C13) for a given amount of carbon input ($\Delta\mathrm{C}_\mathrm{l}$). The equilibrium litter carbon pool size increases with soil temperature, and is independent of carbon input based on Eq. (12) (see Fig. 6d). When soil temperature is low, C_l^* is low, therefore sensitivity of F_B to carbon input is high, or when soil temperature is high, C_l^* is high, the sensitivity of F_B in model B to carbon input is low because of saturating response in the regular Michaelis-Menten equation.

4 Discussion

Here we analysed the responses of different carbon pools to perturbation, soil warming and increased carbon input in two nonlinear microbial soil carbon models. Table 2 listed their key differences of those responses.

Some of those differences also depend on parameter values in each model. For example, there has been a debate about the temperature sensitivities of microbial biomass turnover rate and microbial growth efficiency (Frey et al., 2013; Hargety et al., 2014). If microbial turnover rate is not sensitive to soil temperature and microbial growth efficiency is, as found by Frey et al. (2013), the minimum soil carbon temperature, T_x is about 25 °C for $x = 0.015\,\mathrm{K}^{-1}$ and $a = 0.05$, the values that used by Allison et al. (2010) and German et al. (2012) (see Fig. 3a), then equilibrium soil carbon will decrease over most temperate and boreal regions where mean soil temperature within the rooting zone is below 25 °C for most time of the growing season, and will increase in tropical regions where the mean soil temperature of the top 100 cm soil is close to 25 °C for most time of the year with soil warming. Therefore the simulated responses of equilibrium soil carbon to warming by the two nonlinear models are quite similar in the direction of response over temperate and boreal regions, but different in the tropical regions. However if microbial turnover rate is sensitive to soil temperature and microbial growth efficiency is not, as found by Hargety et al. (2014), then T_x is < 0 °C at $\alpha_s > 0.055$ (°C)$^{-1}$, therefore equilibrium soil carbon will increase in model B, but decrease in model A with warming, therefore the predicted responses of soil carbon to warming by the two nonlinear models differ significantly across all major global biomes where mean rooting zone soil temperature over the growing season is above 0 °C.

Some of the key differences in the responses of the two nonlinear models can be used to differentiate which model is more applicable to the real world using field measurements. For example, the oscillatory response of model A generally is quite small ($< 1\,\%$), which is quite consistent with the results from litter removal experiments (Sayer, Powers and Tanner, 2007 for example). The relatively large and more persistent oscillation in model B has not been observed in the field, and the insensitivity of soil carbon to a perturbation in litter or soil microbial carbon pool in model B also needs to be assessed against long term field experiments such as the DIRT experiment (Nadelhoffer et al., 2004). Model B at its present form may not be applicable to field conditions. It has been argued that the influences of microbial community structure and their activities on mineral soil carbon decomposition at field scale may be much smaller than at rhizosphere (Schimel and Schaeffer, 2012), because substrate concentration rather microbial activity is the rate-limiting step for the decomposition of soil organic matter in mineral soil. A recent study by Sulman et al. (2014) clearly showed the importance of physical protection of microbial by-products in forming stable soil organic matter, and its implication on the response of global soil carbon to carbon input. This mechanism has been recently incorporated into a nonlinear soil microbial carbon model (Wieder et al., 2014). Whether the large oscillatory responses of model B will be significantly damped with the addition of the physical protection mechanism is yet to be studied.

Two models also have quite different sensitivity to soil warming (see Table 2), particularly in the warm regions. Results from a decade-long soil warming experiment showed that warming did not reduce soil carbon, because plant carbon production increased as a result of increased availability of soil mineral nitrogen in that nitrogen-limiting forest (Melillo et al., 2002). However this is quite a different mechanism as represented in model B that does not include nitrogen cycle and the response of carbon input to warming in our study.

Overall both models can simulate the response to carbon input, although model A simulates a lower response than model B and has different sensitivities to carbon input at different soil temperature from model B, particularly under cool climate conditions (see Table 2). So far results from litter manipulation experiments in the field have not been analysed for their sensitivity to soil temperature. The differences in the responses of soil carbon decomposition to an increased carbon input we identified between the two models can also be used to assess which model is more applicable in the field using experiments with different carbon input under cool (mean annual air temperature $< 10\,^{\circ}\mathrm{C}$) and warm (mean annual temperature $> 20\,^{\circ}\mathrm{C}$) conditions. If the sensitivity of soil carbon decomposition to an increased carbon input under cool conditions is greater than that under warm conditions, then model B is more appropriate than model A. This has yet to be tested.

Our analysis here does not include some other key processes, such as the transformations of different forms of organic carbon substrates by different microbial communities as included in some models (see Grant, 2014; Riley et al., 2014 for example), therefore the conclusions from this study about the two nonlinear models should be interpreted with some caution. As shown by Tang and Riley (2014), interactions among soil mineral sorption, carbon substrate and microbial processes can generate transient changes in the apparent sensitivity of soil carbon decomposition to soil temperature, therefore the static dependence of microbial processes on soil temperature as used in our study may not be applicable, and minimum soil carbon temperature as predicted may differ significantly from field observations. Our simplification of different soil microbial community and variable quality of soil carbon as observed in the field is necessary for analytic tractability, but may also limit the applicability of our results to field experiments. For example, Allison (2012) showed that the apparent kinetics of soil carbon decomposition can vary with the spatial scale: regular Michaelis-Menten kinetics at microsite coupled with explicit representation of different strategies for facilitations and competitions among different microbial taxa can generate litter carbon decomposition with a kinetics similar to reverse Michaelis-Menten equation. Therefore the identified differences between the two models should vary with the spatial scale.

Finally both models have a number of parameters, and their values are largely based on laboratory studies (Allison et al., 2010). The values of those parameters may be quite different under field conditions. Evaluation of their applicability under a wide range of field conditions will require an integrated approach, such as applications of model-data fusion using a range of field experiments (Wieder et al., 2015). This will eventually lead a better understanding of the significance of microbial activity on soil carbon decomposition and a more accurate prediction of carbon-climate interaction under future climate conditions.

5 Conclusions

This study analyzed the mathematical properties of two nonlinear microbial soil carbon models and their responses to soil warming and carbon input. We found that the model using the reverse Michaelis-Menten kinetics (model A) has short and more frequent oscillations than the model using regular Michaelis-Menten kinetics (model B) in response to a small perturbation.

The responses of soil carbon to warming can be quite different between the two models. Under global warming, model A always simulates a decrease in soil carbon, but model B will likely simulate a decrease in soil carbon in temperate and boreal region, and an increase in soil carbon in tropical regions, depending on the sensitivities of microbial growth efficiency and microbial biomass turnover rate in model B.

The response to carbon input varies soil temperature in both models. The simulated maximum response to priming by model A generally is smaller than that by model B, because of the faster decline in microbial biomass and rate of SOC decomposition of the control treatments as simulated by model B. The maximum rate of CO_2 efflux from SOC decomposition (F_{max}) to carbon input in the primed treatment depends on initial microbial biomass at steady state in model A, and on the initial litter carbon pool size at steady state in model B, and both dependencies are nonlinear with a saturation response at large microbial biomass or litter carbon pool sizes. Steady state microbial biomass decreases with an increase in soil temperature in both models, and steady state litter carbon increases with an increase in soil temperature, therefore the sensitivity of F_{max} to carbon input increases with an increase in soil temperature until soil temperature is lower than 2× °C in model A, and decreases with an increase in soil temperature in model B.

Based on those differences between the two models, we can design laboratory or field experiments to assess which model is more applicable in real world, therefore advance our understanding of the importance of microbial processes at regional to global scales.

Appendix A: Stability analysis of model A

The Jacobian at the equilibrium pool sizes, J, is given by

$$\mathbf{J} = \begin{pmatrix} -a_1 & -a_3 & 0 \\ \varepsilon a_1 & \varepsilon\left(a_3 + a_4\right) - \mu_\mathrm{b} & \varepsilon a_2 \\ 0 & \mu_\mathrm{b} - a_4 & -a_2 \end{pmatrix} \tag{A1}$$

where $a_1 = \mu_\mathrm{l} g$, $a_2 = \mu_\mathrm{s} g$, $a_3 = \mu_\mathrm{l} \mathrm{C}_\mathrm{l}^* \frac{\partial g}{\partial \mathrm{C}_\mathrm{b}}\Big|_{\mathrm{C}_\mathrm{b}=C_\mathrm{b}^*}$, $a_4 = \mu_\mathrm{s} \mathrm{C}_\mathrm{s}^* \frac{\partial g}{\partial \mathrm{C}_\mathrm{b}}\Big|_{\mathrm{C}_\mathrm{b}=C_\mathrm{b}^*}$, $g = \frac{\mathrm{C}_\mathrm{b}^*}{\mathrm{C}_\mathrm{b}^* + K_\mathrm{b}}$, $\frac{\partial g}{\partial \mathrm{C}_\mathrm{b}}\Big|_{\mathrm{C}_\mathrm{b}=C_\mathrm{b}^*} = \frac{K_\mathrm{b}}{(\mathrm{C}_\mathrm{b}^* + K_\mathrm{b})^2}$, and C_l^*, C_b^* and C_s^* are the equilibrium pool sizes of litter carbon, microbial biomass and soil carbon in $\mathrm{g\,C\,m^{-2}}$, respectively.

Three eigenvalues of J are given by

$$\begin{pmatrix} \lambda_1 \\ \lambda_2 \\ \lambda_3 \end{pmatrix} \approx \begin{pmatrix} \dfrac{-\mathrm{C}_\mathrm{b}^*\left(\mu_\mathrm{b} + \mu_\mathrm{l}\right) + \sqrt{\mathrm{C}_\mathrm{b}^* F_\Delta}}{2(\mathrm{C}_\mathrm{b}^* + K_\mathrm{b})} \\ \dfrac{-\mathrm{C}_\mathrm{b}^*\left(\mu_\mathrm{b} + \mu_\mathrm{l}\right) - \sqrt{\mathrm{C}_\mathrm{b}^* F_\Delta}}{2(\mathrm{C}_\mathrm{b}^* + K_\mathrm{b})} \\ -\mu_\mathrm{s} g \end{pmatrix} \tag{A2}$$

where $F_\Delta = \mathrm{C}_\mathrm{b}^*(\mu_\mathrm{b} - \mu_\mathrm{l})^2 - 4\mu_\mathrm{b}\mu_\mathrm{l}K_\mathrm{b}(1 - \varepsilon)$.

Title Page
Abstract Introduction
Conclusions References
Tables Figures
◀| |▶
◀ ▶
Back Close
Full Screen / Esc
Printer-friendly Version
Interactive Discussion

These three eigenvalues correspond to three carbon pools (λ_1 for litter carbon, λ_2 for microbial biomass and λ_3 for soil carbon). If the eigenvalue of a carbon pool is complex, then the response of that pool to a small perturbation is oscillatory, or monotonic otherwise. If the real part of the eigenvalue is negative, then the response is stable.

Therefore the responses of all three carbon pools to a small perturbation are monotonic if $F_\Delta > 0$, or $F_{\text{npp}} > 4\frac{(1-\varepsilon)^2}{\varepsilon}\frac{\mu_\text{l}\mu_\text{b}^2}{(\mu_\text{b}-\mu_\text{l})^2}K_\text{b}$ or oscillatory otherwise (or $F_\Delta < 0$). The responses of all carbon pools always are stable because $\frac{-\text{C}_\text{b}^*(\mu_\text{b}+\mu_\text{l})}{2(\text{C}_\text{b}^*+K_\text{b})} < 0$.

The corresponding eigenvectors of J are given by

$$\begin{pmatrix} v_1 & v_2 & v_3 \end{pmatrix} \approx \begin{pmatrix} A + B\sqrt{\text{C}_\text{b}^* F_\Delta} & A - B\sqrt{\text{C}_\text{b}^* F_\Delta} & 0 \\ \dfrac{-\text{C}_\text{b}^*(\mu_\text{b}+\mu_\text{l}-2\mu_\text{s}) + \sqrt{\text{C}_\text{b}^* F_\Delta}}{2\mu_\text{b}\text{C}_\text{b}^*} & \dfrac{-\text{C}_\text{b}^*(\mu_\text{b}+\mu_\text{l}-2\mu_\text{s}) - \sqrt{\text{C}_\text{b}^* F_\Delta}}{2\mu_\text{b}\text{C}_\text{b}^*} & 0 \\ 1 & 1 & 1 \end{pmatrix} \tag{A3}$$

where $A = -\frac{(\mu_\text{b}-\mu_\text{l})(\mu_\text{l}-\mu_\text{s})}{2\varepsilon\mu_\text{b}\mu_\text{l}} - (\varepsilon^{-1} - 1)\frac{K_\text{b}}{\text{C}_\text{b}^*}$

$$B = \frac{\mu_\text{l} - \mu_\text{s}}{2\varepsilon\mu_\text{b}\mu_\text{l}\text{C}_\text{b}^*}.$$

When the responses of carbon pools to a small perturbation are oscillatory and stable, the amplitude of oscillation decreases exponentially after $t = 0$. The oscillatory response can be characterized by its half-life ($t_{0.5}$) and period (p) (both in years) calculated from their eigenvalues of J. The amplitude of a stable oscillation decreases exponentially over time, and time when the amplitude is half as much as the amplitude at $t = 0$ is defined as $t_{0.5}$. $t_{0.5}$ and p are calculated as

$$t_{0.5} = -\frac{\ln(2)}{\frac{-C_b^*(\mu_b+\mu_l)}{2(C_b^*+K_b)}} = \frac{2\ln(2)\left(C_b^*+K_b\right)}{C_b^*\left(\mu_b+\mu_l\right)} \tag{A4}$$

$$p = \frac{2\pi}{\frac{\sqrt{-C_b^* F_\Delta}}{2(C_b^*+K_b)}} = \frac{2\pi(C_b^*+K_b)}{\sqrt{-C_b^* F_\Delta}} \tag{A5}$$

for model A. Wang et al. (2014) gave the formulae for $t_{0.5}$ and p for model B (their Eqs. 24 and 25).

As shown in Fig. A1, the half-life is longest for both models when soil temperature is high and carbon input is low, conditions often experienced in arid ecosystems, implying a strong oscillation at these conditions. At a given soil temperature and carbon input, the half-life for model A is about half as much as that for model B (see Fig. A1a and b). When carbon input is $> 1000\,\mathrm{g\,C\,m^{-2}\,year^{-1}}$, as in tropical rainforests, the half-life is less than 1 year for model A at a soil temperature between 20 and 30 °C, and for model B at a soil temperature between 0 and 20 °C only.

Over the range of realistic carbon input and soil temperature, the values of both $t_{0.5}$ and p of model A are less than half as much as those of model B (See Fig. A1). Therefore the responses of carbon pool sizes to a small perturbation in model A oscillate faster and those oscillations also damp faster than model B.

As shown by Wang et al. (2014), the evolution of each carbon pool after a small perturbation can be mathematically represented using the eigenvalues, eigenvectors and initial pool sizes. The third elements of eigenvectors corresponding to litter carbon and microbial biomass represent the influences of those two carbon pools at any time t on soil carbon. Because those elements are nonzero, therefore oscillation of litter carbon and microbial biomass will also cause the response of soil carbon to be oscillatory, although the oscillation is small and damps very quickly. In model B, the third elements of the eigenvectors corresponding to litter carbon and microbial biomass zero, therefore oscillatory responses of litter carbon and microbial biomass have no effect on the response of soil carbon, and the eigenvalue of the soil carbon in model B is negative real, therefore the response of soil carbon to a small perturbation always is monotonic and stable in model B (see Appendix A in Wang et al., 2014).

Appendix B: Soil temperature at which equilibrium soil carbon pool is minimum (T_x)

The steady state soil carbon pool size of model A is

$$\mathrm{C}_\mathrm{s}^* = \left(a + \frac{1}{\varepsilon^{-1}-1}\right)\frac{F_\mathrm{npp}}{\mu_\mathrm{s}} + \left(1 + a\left(\varepsilon^{-1}-1\right)\right)\frac{\mu_\mathrm{b} K_\mathrm{b}}{\mu_\mathrm{s}} \tag{B1}$$

The first term on the right-hand side of Eq. (B1) always decreases with an increase in T_s, and the second term has two parts: $\left(1 + a\left(\varepsilon^{-1}-1\right)\right)$ and $\frac{\mu_\mathrm{b} K_\mathrm{b}}{\mu_\mathrm{s}}$. Because Both K_b and μ_s increase with T_s exponentially, and the sensitivity μ_s to T_s is much greater than K_b, therefore $\frac{K_\mathrm{b}}{\mu_\mathrm{s}}$ always decreases with an increase in T_s, and that decrease is much greater than the increase in $\left(1 + a\left(\varepsilon^{-1}-1\right)\right)$ with T_s, therefore the second term also decreases with an increase in soil temperature, independent of temperature sensitivity of μ_b. In summary for model A, $\frac{\mathrm{dC}_\mathrm{s}^*}{\mathrm{d}T_\mathrm{s}} < 0$.

The steady state pool of soil carbon in model B is

$$\mathrm{C}_\mathrm{s}^* = \frac{K_\mathrm{s}}{\frac{V_\mathrm{s}}{\mu_\mathrm{b}}\frac{\varepsilon}{\varepsilon+a(1-\varepsilon)} - 1} \tag{B2}$$

Assuming that $\frac{V_\mathrm{s}}{\mu_\mathrm{b}}\frac{\varepsilon}{\varepsilon+a(1-\varepsilon)} \gg 1$, we can therefore approximate C_s^* as

$$\mathrm{C}_\mathrm{s}^* \approx \frac{K_\mathrm{s}}{\frac{V_\mathrm{s}}{\mu_\mathrm{b}}\frac{\varepsilon}{\varepsilon+a(1-\varepsilon)}} = \frac{K_\mathrm{sR}\mu_\mathrm{bR}}{V_\mathrm{sR}} \exp\left[(\beta_\mathrm{k} + b - \beta_\mathrm{v})(T_\mathrm{s} - T_\mathrm{R})\right]\left[1 + a\left(\frac{1}{\varepsilon_0 - x\,(T_\mathrm{s} - T_\mathrm{R})} - 1\right)\right] \tag{B3}$$

It can be easily shown that T_x can only exist only when $\beta_\mathrm{k} + b - \beta_\mathrm{v} \le 0$ and $0 < a < 1$ and

$$T_x = T_\mathrm{R} + \frac{\varepsilon_0 - z}{x} \tag{B4}$$

$$\beta_\mathrm{k} + b - \beta_\mathrm{v} z = -0.5\frac{a}{1-a} + 0.5\sqrt{\left(\frac{a}{1-a}\right)^2 - 4\left(\frac{a}{1-a}\right)\frac{x}{\beta_\mathrm{k} + b - \beta_\mathrm{v}}} \tag{B5}$$

when $a = 0$, T_x does not exist and

$$\frac{\mathrm{d}C_\mathrm{s}^*}{\mathrm{d}T_\mathrm{s}} < 0; \quad \text{when } \beta_\mathrm{k} + b - \beta_\mathrm{v} \le 0; \tag{B6}$$

$$\frac{\mathrm{d}C_\mathrm{s}^*}{\mathrm{d}T_\mathrm{s}} > 0; \quad \text{when } \beta_\mathrm{k} + b - \beta_\mathrm{v} > 0 \tag{B7}$$

for model B.

Appendix C: Derivation of analytic approximation for timing and magnitude of maxim microbial biomass after priming

Both models can be used to simulate the response of soil carbon to priming by specifying different initial pool sizes for the primed and control treatments. The initial values are

$C_\mathrm{l}(t=0) = C_\mathrm{l}^* + \Delta C_\mathrm{l}$; $C_\mathrm{b}(t=0) = C_\mathrm{b}^*$ and $C_\mathrm{s}(t=0) = C_\mathrm{s}^*$ for priming treatment;
$C_\mathrm{l}(t=0) = C_\mathrm{l}^*$; $C_\mathrm{b}(t=0) = C_\mathrm{b}^*$ and $C_\mathrm{s}(t=0) = C_\mathrm{s}^*$ for the control.

Here we assume that all pools are at equilibrium just before the priming treatment at $t = 0$. C_l^*, C_b^* and C_s^* are equilibrium pool sizes, and ΔC_l is the amount of litter carbon added at time $t = 0$. No carbon is added to both treatments after $t = 0$.

The CO_2 efflux from soil carbon decomposition is calculated using Eq. (15) for model A and Eq. (16) for model B. Therefore we need to solve the three equations for C_b and C_s for $t > 0$. Observations show that maximum priming response occurs soon after priming treatment (Kuzyakova, Friedelb and Stahr, 2000), therefore maximum priming response can be considered as a short-time scale phenomenon. At short-time scale, C_s can be considered as being constant, and the maximum CO_2 efflux from the priming treatment will occur when the microbial biomass reaches maximum after $t = 0$. Therefore we will use a second-order Taylor expansion to obtain the approximate solutions to the timing and magnitude of maximum CO_2 efflux from the soil carbon decomposition in the priming treatment for each model.

For model A, Eqs. (1) and (2) for both treatments after $t > 0$ becomes

$$\frac{dC_l}{dt} = -\mu_l C_l \frac{C_b}{C_b + K_b} \tag{C1}$$

$$\frac{dC_s}{dt} = \mu_b C_b - \mu_s C_s \frac{C_b}{C_b + K_b}$$

As the litter pool size at time $t = 0$ is above its equilibrium value, therefore the microbial biomass will likely increase after $t = 0$ and then reaches its maximum value, and then decline.

Equations (C1), (2) and (3) can be simplified using variable substitution.

Let

$$\widetilde{C}_b = \frac{C_b}{K_b}, \widetilde{C}_l = \frac{C_l}{K_b}\frac{\mu_l}{\mu_b}\widetilde{C}_s = \frac{C_s}{K_b}\frac{\mu_s}{\mu_b}\Delta\widetilde{C}_l = \frac{\Delta C_l}{K_b}\frac{\mu_l}{\mu_b}\tau = t\mu_b, a_1 = \frac{\mu_l}{\mu_b}a_2 = \frac{\mu_s}{\mu_b}, a_3 = \frac{F_{NPP}\mu_l}{K_b\mu_b^2}$$

Then those three equations can be written as

$$\frac{d\widetilde{C}_l}{d\tau} = -a_1\widetilde{C}_l\frac{\widetilde{C}_b}{\widetilde{C}_b+1} \tag{C2}$$

$$\frac{d\widetilde{C}_s}{d\tau} = a_2(\widetilde{C}_b - \widetilde{C}_s\frac{\widetilde{C}_b}{\widetilde{C}_b+1}) \tag{C3}$$

$$\frac{d\widetilde{C}_b}{d\tau} = \varepsilon(\widetilde{C}_l + \widetilde{C}_s)\frac{\widetilde{C}_b}{\widetilde{C}_b+1} - \widetilde{C}_b \tag{C4}$$

with the initial pool sizes of $\widetilde{C}_b(0) = \frac{a_3}{a_1}\frac{\varepsilon}{1-\varepsilon}$, $\widetilde{C}_s(0) = \frac{a_3}{a_1}\left(\frac{\varepsilon}{1-\varepsilon} + a\right) + 1 + a\frac{1-\varepsilon}{\varepsilon}$ for both treatments, and $\widetilde{C}_l(0) = (1-a)(\frac{a_3}{a_1} + \frac{1-\varepsilon}{\varepsilon}) + \Delta\widetilde{C}_l$ for the primed treatment; and $\widetilde{C}_l(0) = (1-a)(\frac{a_3}{a_1} + \frac{1-\varepsilon}{\varepsilon})$ for the control treatment.

At relatively short-time scale, $a_2 \ll 1$, therefore $\widetilde{C}_s(t) \rightarrow \widetilde{C}_s(t=0)$ Microbial biomass carbon after $t = 0$ can be approximated using the second-order Taylor expansion. That is:

$$\widetilde{C}_b(t) = \widetilde{C}_b(0) + t\widetilde{C}'_b(0) + \frac{t^2}{2}\widetilde{C}''_b(0) \tag{C5}$$

Assuming that $t = t_{\text{max,A}}$, $\widetilde{C}_b$ is maximum, then $\widetilde{C}'_b\left(t_{\text{max,A}}\right) = 0$. Equation (C5) becomes

$$\widetilde{C}'_b\left(t_{max,A}\right) = \widetilde{C}'_b(0) + t_{max,A}\widetilde{C}''_b(0) = 0 \tag{C6}$$

Both $\widetilde{C}'_b(0)$ and $\widetilde{C}''_b(0)$ can be obtained differentiating Eq. (C4) at $t = 0$. We have

$$\widetilde{C}'_b(0) = \varepsilon\frac{\widetilde{C}_b(0)}{1+\widetilde{C}_b(0)}\Delta\widetilde{C}_l \tag{C7}$$

$$\widetilde{C}''_b(0) = -\varepsilon\frac{\widetilde{C}_b(0)}{1+\widetilde{C}_b(0)}\Delta\widetilde{C}_l((1-a)\frac{a_3}{\Delta\widetilde{C}_l} + (1+a_1)\frac{\widetilde{C}_b(0)}{1+\widetilde{C}_b(0)} - \frac{\varepsilon\Delta\widetilde{C}_l}{(1+\widetilde{C}_b(0))^2}) \tag{C8}$$

Substituting Eqs. (C7) and (C8) into (C6), and solving for $t_{\mathrm{max,A}}$, we have

$$t_{\mathrm{max,A}} = -\frac{1}{\mu_\mathrm{b}}\frac{\widetilde{\mathrm{C}}'_\mathrm{b}(0)}{\widetilde{\mathrm{C}}''_\mathrm{b}(0)} = \frac{1}{(1-a)\frac{F_\mathrm{npp}}{\Delta \mathrm{C}_\mathrm{l}} + (\mu_\mathrm{b}+\mu_\mathrm{l})\frac{\mathrm{C}_\mathrm{b}^*}{\mathrm{C}_\mathrm{b}^*+K_\mathrm{b}} - \frac{\varepsilon K_\mathrm{b}\mu_\mathrm{l}\Delta \mathrm{C}_\mathrm{l}}{(\mathrm{C}_\mathrm{b}^*+K_\mathrm{b})^2}} \tag{C9}$$

Substituting Eq. (C9) into (C5), we have the maximum microbial biomass at $t_{\mathrm{max,A}}$, or $\mathrm{C}_{\mathrm{bmax,A}}$ for the primed treatment as follows:

$$\mathrm{C}_{\mathrm{bmax,A}} = K_\mathrm{b}\widetilde{\mathrm{C}}_\mathrm{b}\left(t_{max,A}\right) = \mathrm{C}_\mathrm{b}^* + \frac{t_{max,A}}{2}\frac{\varepsilon \mathrm{C}_\mathrm{b}^*}{\mathrm{C}_\mathrm{b}^*+K_\mathrm{b}}\mu_\mathrm{l}\Delta \mathrm{C}_\mathrm{l} \tag{C10}$$

The maximum rate of $\mathrm{CO_2}$ release from decomposition of soil organic carbon, $F_{\mathrm{CO_2}}$ at $t = t_{\mathrm{max,A}}$ is given by

$$F_\mathrm{A} = (1-\varepsilon)\,\mu_\mathrm{s}\mathrm{C}_\mathrm{s}\frac{\mathrm{C}_{\mathrm{bmax,A}}}{\mathrm{C}_{\mathrm{bmax,A}}+K_\mathrm{b}}. \tag{C11}$$

Similarly we derived the approximations for the timing ($t_{\mathrm{max,B}}$) and magnitude of maximum microbial biomass ($\mathrm{C}_{\mathrm{bmax,B}}$) in the primed treatment at $t > 0$. They are

$$t_{\mathrm{max,B}} = \frac{1}{\frac{\varepsilon K_\mathrm{l}\mathrm{C}_\mathrm{b}^*}{(\varepsilon M_\mathrm{l}-(1-a)(1-\varepsilon)\mu_\mathrm{b})}\frac{(\mathrm{C}_\mathrm{L}^*+\Delta \mathrm{C}_\mathrm{l})(V_\mathrm{l})^2}{(\mathrm{C}_\mathrm{L}^*+\Delta \mathrm{C}_\mathrm{l}+K_\mathrm{l})^3} - (\varepsilon M_\mathrm{l}-(1-a)(1-\varepsilon)\,\mu_\mathrm{b})} \tag{C12}$$

$$\mathrm{C}_{\mathrm{bmax,B}} = \mathrm{C}_\mathrm{b}^*\left(1+0.5t_{\mathrm{max,B}}\,(\varepsilon M_\mathrm{l}-(1-a)\,(1-\varepsilon)\,\mu_\mathrm{b})\right) \tag{C13}$$

where

$$M_\mathrm{l} = \frac{V_\mathrm{l}\left(\mathrm{C}_\mathrm{l}^*+\Delta \mathrm{C}_\mathrm{l}\right)}{\mathrm{C}_\mathrm{l}^*+\Delta \mathrm{C}_\mathrm{l}+K_\mathrm{l}}$$

The rate of CO_2 release from decomposition of soil carbon, F_B, for model B at time $t = t_{max,B}$ is given by

$$F_B = (1-\varepsilon)\, C_{bmax,B} \frac{V_s C_s}{C_s + K_s} \approx (1-\varepsilon)\, \mu_b C_{bmax,B}. \tag{C14}$$

Comparison with numerical simulations show that the relative error of Eq. (C11) is $< 3\,\%$ across soil temperature and carbon input within their realistic ranges. However errors in Eq. (C14) for model 2 can be quite large, particularly at high carbon input. Equation (C14) is only reasonably accurate (relatively error $< 10\,\%$) at low carbon input $< 700\,\mathrm{g\,C\,m^{-2}}$.

Acknowledgements. This work was assisted through participation of the authors in the working group Nonautonomous Systems and Terrestrial Carbon Cycle, at the National Institute for Mathematical and Biological Synthesis, an institute sponsored by the National Science Foundation, the US Department of Homeland Security, and the US Department of Agriculture through NSF award no. EF-0832858, with additional support from The University of Tennessee, Knoxville. We are grateful for the constructive comments from the associate editor and three reviewers. Sources codes and data used in this study are available on request by email (yingping.wang@csiro.au).

References

Allison, S. D.: A trait-based approach for modelling microbial litter decomposition, Ecol. Lett., 15, 1058–1070, 2012.

Allison, S. D., Wallenstein, M. D., and Bradford, M. A.: Soil-carbon response to warming dependent on microbial physiology, Nature Geosci., 3, 336–340, 2010.

Bradford, M. A., Davies, C. A., Frey, S. D., Maddox, T. R., Melillo, J. M., Mohan, J. E., Reynolds, J. F., Treseder, K. K., and Wallenstein, M. D.: Thermal adaptation of soil microbial respiration to elevated temperature, Ecol. Lett., 11, 1316–1327, 2008.

Cavelier, J.: Fine-root biomass and soil properties in a semideciduous and a lower montan rain forest in Panama, Plant Soil, 142, 187–201, 1992,

Cheng, W., Parton, W. J., Gonzalez-Meler, M. A., Phillips, R., Asao, S., McNickle, G. G., Brzostek, E., and Jastrow, J. D.: Synthesis and modeling perspectives of rhizosphere priming, New Phytol., 201, 31–44, 2014.

Drake, J. E., Darby, B. A., Giasson, M. A., Kramer, M. A., Phillips, R. P., and Finzi, A. C.: Stoichiometry constrains microbial response to root exudation- insights from a model and a field experiment in a temperate forest, Biogeosciences, 10, 821–838, doi:10.5194/bg-10-821-2013, 2013.

Drazin, P. G.: Nonlinear Systems, Cambridge University Press, Cambridge, p. 317, 1992.

Fontaine, S. and Barot, S.: Size and functional diversity of microbe populations control plant persistence and long-term soil carbon accumulation, Ecol. Lett., 8, 1075–1087,2005.

Fontaine, S., Bardoux, G., Abbadie, L., and Mariotti, A.: Carbon input to soil may decrease soil carbon content, Ecol. Lett., 7, 314–320, 2004.

Fontaine, S., Barot, S., Barre, P., Bdioui, N., Mary, B., and Rumpel, C.: Stability of organic carbon in deep soil layers controlled by fresh carbon supply, Nature, 450, 277–281, 2007.

Frey, S. D., Lee, J., Melillo, J. M., and Six, J.: The temperature response of soil microbial efficiency and its feedback to climate, Nature Climate Change, 3, 395–398, 2013.

Fujita, Y., Witte, J. M., and van Bodegom, P. M.: Incorporating microbial ecology concepts into global soil mineralization models to improve predictions of carbon and nitrogen fluxes, Global Biogeochem. Cy., 28, 223–238, 2014.

German, D. P., Marcelo, K. R. B., Stone, M. M., and Allison, S. D.: The Michaelis–Menten kinetics of soil extracellularenzymes in response to temperature: a cross-latitudinal study, Glob. Change Biol., 18, 1468–1479, 2012.

Grant, R. F.: Nitrogen mineralization drives the response of forest productivity to soil warming: Modelling in ecosys vs. measurements from the Harvard soil heating experiment, Ecol. Modell., 288, 38–46, 2014.

Grimm, R.: Soil-landscape modelling of Barro Colorado Island with special emphasis on soil organic carbon and clay mineralogy, University of Posdam, Posdam, Germany, 2007.

Hagerty, S. B., van Groenigen, K. J., Allison, S. D., Hungate, B. A., Schwartz, E., Koch, G. W., Kolka, R. K., and Dijkstra, P.: Accelerated microbial turnover but constant growth efficiency with warming in soil, Nature Climate Change, 4, 903–906, 2014.

Jenkinson, D. S, Fox, R. H., and Rayner, J. H.: Interactions between fertilizer nitrogen and soil nitrogen-the so-called "priming" effect, J. Soil Sci., 36, 425–444, 1985.

Jenkinson, D. S., Adams, D. E., and Wild, A.: Model estimates of CO_2 emissions from soil in response to global warming, Nature, 351, 304–306, 1991.

Jones, C. and Falloon, P.: Sources of uncertainties in global modelling of future soil organic carbon storage, in: Uncertainties in Environmental Modelling and Consequences for Policy Making, The NATO Science for Peace and Security Programme, Springer, 283–315, 2009.

Kuzyakova, Y., Friedelb, J. K., and Stahr, K.: Review of mechanisms and quantification of priming effects, Soil Biol. Biochem., 32, 1485–1498, 2000.

Li, J. W., Wang, G., Allison, S. D., Mayes, M. A., and Luo, Y. Q.: Soil carbon sensitivity to temperature and carbon use efficiency compared across microbial-ecosystem models of varying complexity, Biogeochemistry, 119, 67–84, 2014.

Luo, Y. Q., Wan, S. Q., Hui, D. F., and Wallace, L. L.: Acclimatization of soil respiration to warming in a tall grass prairie, Nature, 413, 622–625, 2001.

Manzoni, S. and Porporato, A.: A theoretical analysis of nonlinearities and feedbacks in soil carbon and nitrogen cycles, Soil Biol. Biochem., 39, 1542–1556, 2007.

Manzoni, S., Porporato, A., D'Odorico, P., Laio, F., and Rodriguez-Iturbe, I.: Soil nutrient cycles as a nonlinear dynamic system, Nonl. Proc. Geophys., 11, 589-598, 2004.

Melillo J. M., Steudler, P. A., Aber, J. D., Newkirk, K., Lux, H., Bowles, F. bP., Catricala, C., Magill, A., Ahrens, T., and Morrisseau, S.: Soil warming and carbon-cycle feedbacks to the climate System, Science, 298, 2173–2176, 2002.

Nadelhoffer, K. bJ., Boone, R. D., Bowden, R. D., Canary, J., Kaye, J., Micks, P., Ricca, A., Mcdowell, W., and Aitkenhead, J.: The DIRT experiment, Litter and root influences on forest soil organic matter stocks and function, in: Forests in Time, edited by: Foster, D. R. and Aber, J. D., Yale University Press, New Haven, 2004.

Parnas, H.: Model for decomposition of organic material by microorganisims, Soil Biol. Biochem., 7, 161–169, 1978.

Parnas, H.: A theoretical explanation of the priming effect based on microbial growth with two limiting substrates, Soil Biology and Biochemistry, 8, 139–144, 1979.

Raupach, M. R.: Dynamics of resource production and utilisation in two-component biosphere-human and terrestrial carbon systems, Hydrol. Earth Syst. Sci., 11, 875–889, doi:10.5194/hess-11-875-2007, 2007.

Riley, W. J., Maggi, F., Kleber, M., Torn, M. S., Tang, J. Y., Dwivedi, D., and Guerry, N.: Long residence times of rapidly decomposable soil organic matter: application of a multi-phase, multi-component, and vertically resolved model (BAMS1) to soil carbon dynamics, Geosci. Model Dev., 7, 1335–1355, doi:10.5194/gmd-7-1335-2014, 2014.

Sayer E. J. and Tanner, E. V. J.: Experimental investigation of importance of litterfall in lowland semi-evergreen tropical forest nutrient cycling, J. Ecol., 98, 1052–1062, 2010a.

Sayer E. J. and Tanner, E. V. J.: A new approach to trenching experiments for measuring root-rhizopshere respiration ina lowland tropical forest, Soil Biol. Biochem., 42, 347–352, 2010b.

Sayer, E. J., Powers, J. S., and Tanner, E. V. J.: Increased litterfall in tropical forests boosts the transfer of soil CO_2 to the atmosphere, PLoS ONE, 2, e1299, doi:10.1371/journal.pone.0001299, 2007.

Sayer, E. J., Heard, M. S., Grant, H. K., Marthews, T. R., and Tanner, E. V. J.: Soil carbon release enhanced by increased tropical forest litterfall, Nature Climate Change, 1, 304–307, 2011.

Schimel, J. P. and Schaeffer, S. M.: Microbial control over carbon cycling in soil, Front. Microbiol., 348, 1–11, doi:10.3389/fmicb.2012.00348, 2012.

Schimel, J. P. and Weintraub, M. N.: The implications of exoenzyme activity on microbial carbon and nitrogen limitation in soil: a theoretical model, Soil Biol. Biochem., 35, 549–563, 2003.

Smith, O. L.: An analytic model of the decomposition of soil organic matter, Soil Biol. Biochem., 11, 585–505, 1979

Sulman, B. N., Phillips, R. P., Oishi, A. C., Shevliakova, E., and Pacala, S. W.: Microbe driven turnover offsets mineral-mediated storage of soil carbon under elevated CO_2, Nature Climate Change, 4, 1099–1102, 2014.

Tang, J. and Riley, W.: Weaker soil carbon-climate feedbacks resulting from microbial and abiotic interactions, Nature Climate Change, 5, 56–60, 2014

Wang, Y. P., Chen, B. C., Wieder, W. R., Leite, M., Medlyn, B. E., Rasmussen, M., Smith, M. J., Agusto, F. B., Hoffman, F., and Luo, Y. Q.: Oscillatory behavior of two nonlinear microbial models of soil carbon decomposition, Biogeosciences, 11, 1817–1831, doi:10.5194/bg-11-1817-2014, 2014.

Wieder, W. R., Bonan, G. B., and Allison, S. D.: Global soil carbon projections are improved by modeling microbial processes, Nature Climate Change, 3, 909–912, 2013.

Wieder, W. R., Grandy, A. S., Kallenbach, C. M., and Bonan, G. B.: Integrating microbial physiology and physio-chemical principles in soils with the MIcrobial-MIneral Carbon Stabilization (MIMICS) model, Biogeosciences, 11, 3899–3917, doi:10.5194/bg-11-3899-2014, 2014.

Wieder, W. R., Allison, S. D., Davidson, E. A., Georgiou, K., Harauk, O., He, Y., Hopkins, F., Luo, Y., Smith, M., Sulman, B., Todd-Brown, K., Wang, Y.-P., Xia, J., ans Xu, X.: Explicitly representing soil microbial processes in earth system models, Global Biogeochem. Cy., accepted, 2015.

Wutzler, T. and Reichstein, M.: Colimitation of decomposition by substrate and decomposers – a comparison of model formulations, Biogeosciences, 5, 749–759, doi:10.5194/bg-5-749-2008, 2008.

Wutzler, T. and Reichstein, M.: Priming and substrate quality interactions in soil organic matter models, Biogeosciences, 10, 2089–2103, doi:10.5194/bg-10-2089-2013, 2013.

Table 1. Default values of model parameters and their temperature sensitivities (°C^{-1}).

Default value	Source	Temperature sensitivity	Source
$\varepsilon_\mathrm{R} = 0.39$	Allison et al. (2010)	$x = 0.016$	Allison et al. (2010)
$\mu_\mathrm{bR} = 1.1\ \mathrm{year}^{-1}$	This study	$b = 0.063$	Hagerty et al. (2014)
$\mu_\mathrm{lR} = 0.84\ \mathrm{year}^{-1}$	This study	$\alpha_\mathrm{l} = 0.063$	Hagerty et al. (2014)
$\mu_\mathrm{sR} = 0.028\ \mathrm{year}^{-1}$	This study	$\alpha_\mathrm{s} = 0.063$	Hagerty et al. (2014)
$K_\mathrm{bR} = 100\ \mathrm{g\,C\,m}^{-2}$	This study	$\alpha_\mathrm{k} = 0.007$	Allison et al. (2010)
$K_\mathrm{lR} = 67275\ \mathrm{g\,C\,m}^{-2}$	Wang et al. (2014)	$\beta_\mathrm{kl} = 0.007$	Allison et al. (2010)
$K_\mathrm{sR} = 363871\ \mathrm{g\,C\,m}^{-2}$	Wang et al. (2014)	$\beta_\mathrm{kss} = 0.007$	Allison et al. (2010)
$V_\mathrm{lR} = 172\ \mathrm{year}^{-1}$	Wang et al. (2014)	$\beta_\mathrm{vl} = 0.063$	Allison et al. (2010)
$V_\mathrm{sR} = 32\ \mathrm{year}^{-1}$	Wang et al. (2014)	$\beta_\mathrm{vs} = 0.063$	Allison et al. (2010)

Table 2. Key differences between the two nonlinear soil microbial models.

Response to	Model A	Model B
Pool size perturbation	More frequent and faster damped oscillation in litter and microbial carbon pools; Soil carbon pool may oscillate	Less frequent and slower damped oscillation in litter and microbial carbon pools; Soil carbon pool does not oscillate
Warming	Soil carbon pool always decreases	Soil carbon may increase or decrease
Carbon input	Sensitivity of maximum CO_2 efflux increases with soil temperature	Sensitivity of maximum CO_2 efflux decreases with soil temperature

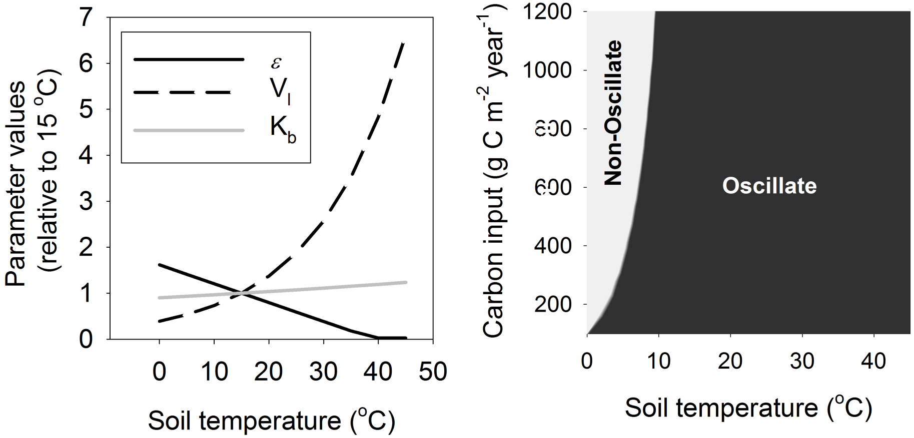

Figure 1. Variation of microbial growth efficiency (ε), V_l and K_b with soil temperature (left panel) or the region in which model A has oscillatory or non-oscillatory response to a small perturbation (right panel) at different carbon input and soil temperature.

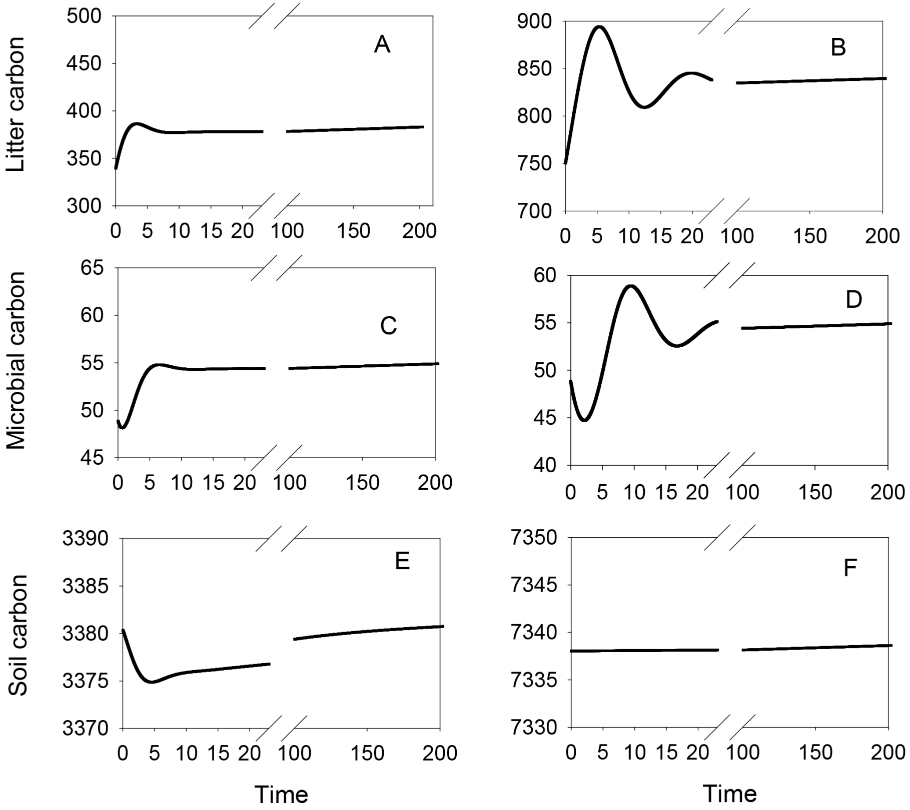

Figure 2. Dynamics of litter carbon **(a, b)** microbial carbon **(c, d)** or soil carbon **(e, f)** for model A (**a, c** and **e**) or model B (**b, d** and **f**) after a 10 % reduction of initial pool size in litter and microbial carbon. The unit is g C m^{-2} for carbon pool on y-axis and year for time. All initial pools are steady state values for a carbon input of 200 g C m^{-2} year^{-1} at a soil temperature is 25 °C.

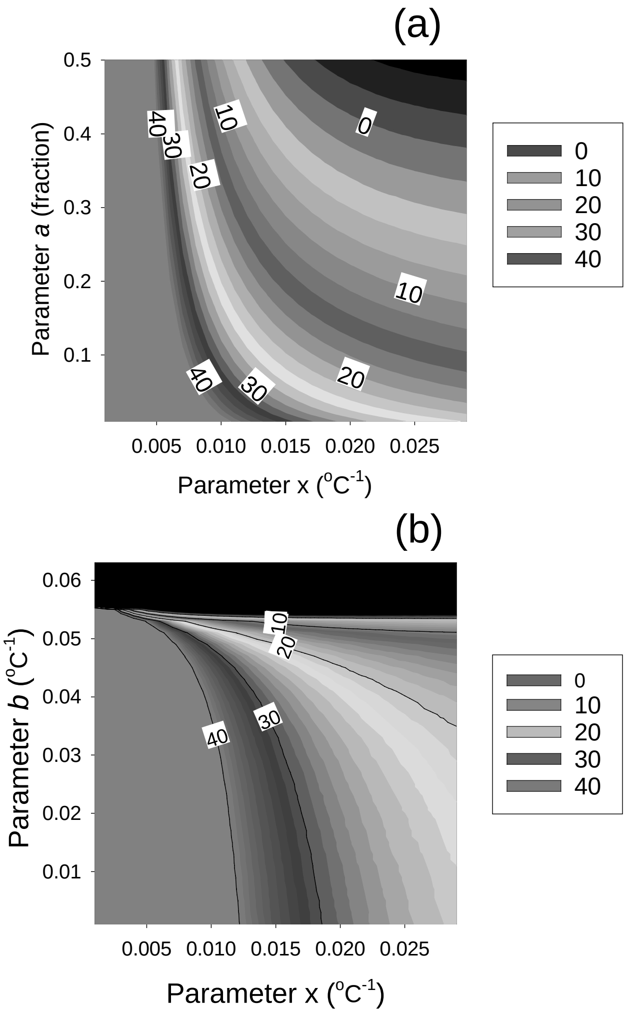
(a)
Parameter a (fraction)
0.5
0.4
0.3
0.2
0.1
0.005 0.010 0.015 0.020 0.025
Parameter x (°C-1)
40
30
20
10
0
10
40
30
20
0
10
20
30
40
(b)
Parameter b (°C-1)
0.06
0.05
0.04
0.03
0.02
0.01
0.005 0.010 0.015 0.020 0.025
Parameter x (°C-1)
10
20
40
30
0
10
20
30
40

Figure 3. **(a)** Variation of minimum soil carbon temperature (T_x) at which equilibrium soil carbon pool size is minimum with the temperature sensitivity of microbial growth efficiency (x), fraction of carbon input directly into soil carbon pool (a). μ_b was fixed at 1.1 year^{-1} (or $b = 0$); **(b)** variation of T_x with x and b. Parameter a was fixed at 0.05 in the simulation. The unit is °C for all the numbers along the contour lines in both **(a)** and **(b)**.

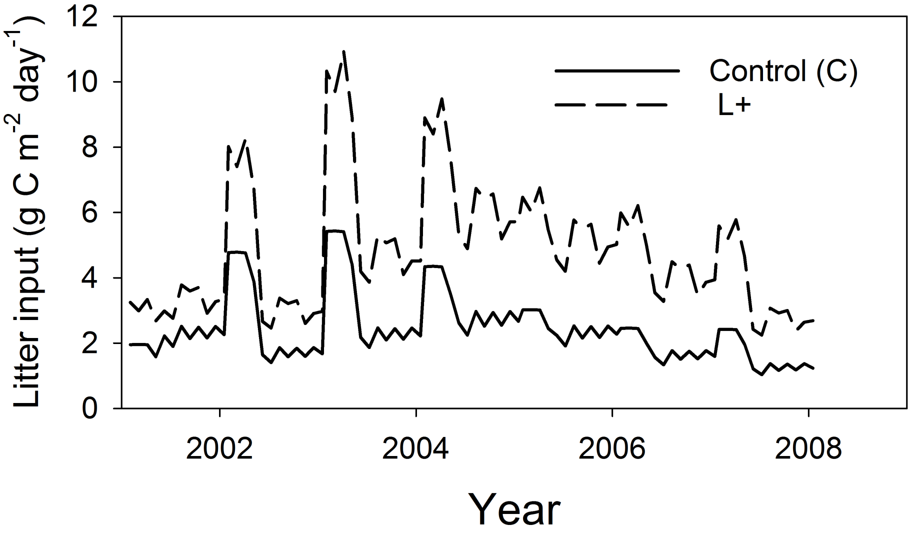

Figure 4. Mean monthly total (above and belowground) litter carbon input to the control or litter addition treatment.

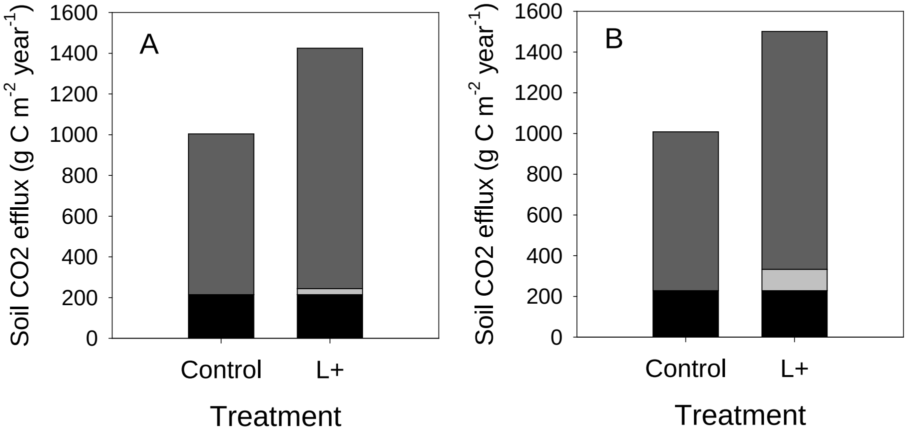

Figure 5. Simulated response of soil CO_2 efflux in control and litter addition (L+) experiments as described by Sayer et al. (2014) using model A **(a)** or B **(b)**. The dark grey bar and black bars represent CO_2 effluxes from litter and soil organic carbon decomposition, respectively. The light grey bar for the litter addition treatment represents the additional CO_2 efflux from soil organic carbon decomposition due to additional litter input.

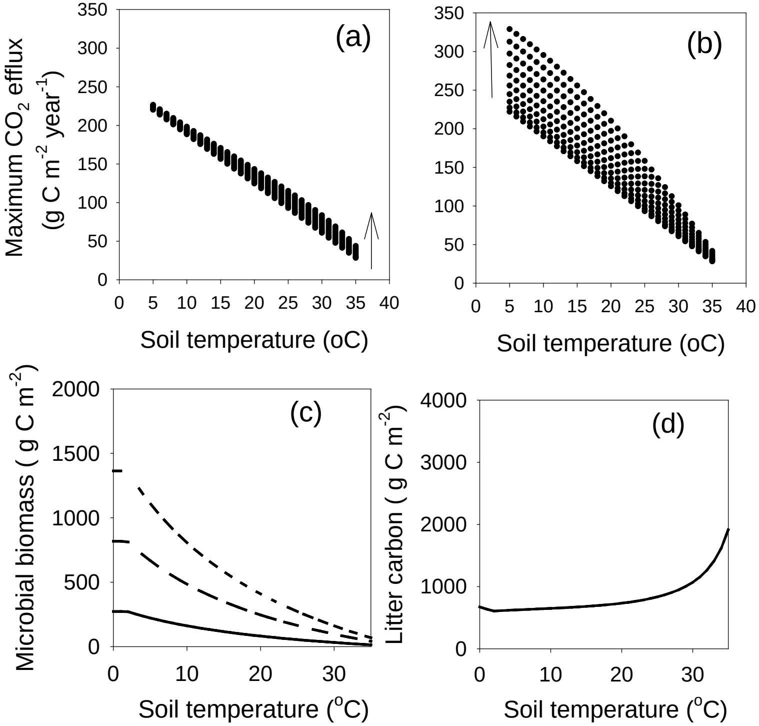

Figure 6. Dependence of maximum rate of CO2 efflux from the decomposition of soil carbon in the primed treatment (F_{max}) as a function of soil temperature and carbon addition at time $t = 0$ for model A **(a)** or B **(b)**. At each soil temperature, the carbon input was varied from 100 g C m^{-2} to 1000 g C m^{-2}, and F_{max} increases with an increase in carbon input as shown by the arrow in each plot. **(c)** Variation of equilibrium soil microbial biomass with soil temperature and carbon input at 200 (solid black), 600 (long shaded) and 1000 (short-dashed) g C m^{-2} year^{-1} for both models; and **(d)** variation of equilibrium litter carbon with soil temperature in model B.

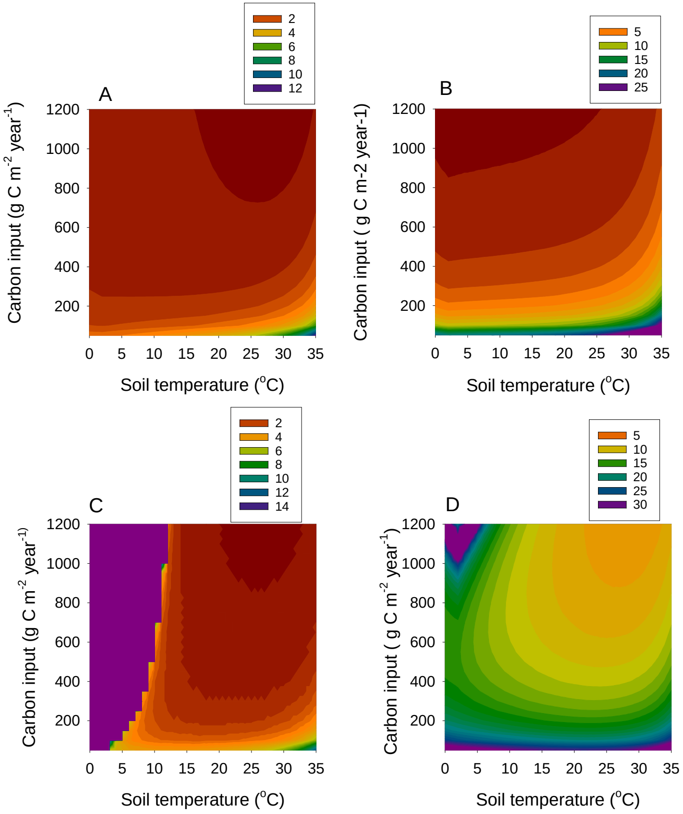

Figure A1. Half-time (**a** and **b**) or period (**c** and **d**) for model A (**a** and **c**) or **(b)** (**b** and **d**). The unit is year for both half-time and period. Note the difference scales used for model A from model B for both half-time and period. The purple region represents non-oscillatory region for model A in **(c)**, and a period greater than 30 years for model B in **(d)**. We assumed that $a = 0$ for all calculations.